

Top squark and neutralino decays in a R-parity violating model constrained by neutrino oscillation data

Siba Prasad Das^{a, 1}, Amitava Datta^{b, 2}, and Sujoy Poddar^{b, 3}

^a*Department of Physics, University of Calcutta, Kolkata- 700 009, India*

^b*Department of Physics, Jadavpur University, Kolkata- 700 032, India*

Abstract

In a R-parity violating (RPV) model of neutrino mass with three bilinear couplings μ_i and three trilinear couplings λ'_{i33} , where i is the lepton index, we find six generic scenarios each with a distinctive pattern of the trilinear couplings consistent with the oscillation data. These patterns may be reflected in direct RPV decays of the lighter top squark or in the RPV decays of the lightest superparticle, assumed to be the lightest neutralino. Typical signal sizes at the Tevatron RUN II and the LHC have been estimated and the results turn out to be encouraging.

PACS numbers: 11.30.Pb, 13.85.-t, 14.60.Pq, 14.80.Ly

¹*spd@juphys.ernet.in*

²*adatta@juphys.ernet.in*

³*sujoy@juphys.ernet.in*

1. Introduction

Neutrino oscillations have been observed in different experiments [1], from which it is confirmed that the neutrinos have tiny masses, several orders of magnitude smaller than any other fermion mass in the Standard Model (SM). If right handed neutrinos are introduced in the SM one can formally get Dirac masses of the neutrinos. But the corresponding Yukawa couplings must be unnaturally small.

The SM being unable to naturally explain the origin of very small neutrino masses , R-parity violating (RPV) supersymmetry (SUSY) [2, 3] could be a viable alternative. In the lepton number violating version of these models, the neutrino masses (Majorana type) and mixing angles [4, 5] can naturally arise without requiring the right handed neutrinos.

In the minimal supersymmetric extension of the SM (MSSM) there is also a R-parity conserving (RPC) sector with Yukawa like couplings and soft breaking masses/ mass parameters, which govern the masses of the superpartners of the SM particles (the sparticles). As demanded by the naturalness argument, these masses should be of the order of one TeV. The theoretical predictions for the neutrino masses and mixing angles depend on these RPC parameters, in addition to the parameters of the RPV sector. Thus the exciting program of sparticle searches and the reconstruction of their masses at the on going (Tevatron RUN II) and the upcoming (the Large Hadron Collider (LHC) or the International Linear Collider (ILC)) accelerator experiments have the potential of testing the RPV models of ν - mass.

In R-parity conserving(RPC) SUSY the lightest supersymmetric particle (LSP) is predicted to be stable and a carrier of missing transverse energy (\cancel{E}_T). In contrast the model under consideration allows the LSP to decay via RPV couplings into lepton number violating modes. The multiplicity of particles in any event is, therefore, much larger compared to the corresponding event in RPC SUSY containing the stable LSP leading to distinct collider signatures. Moreover, since the LSP is not necessarily a carrier of \cancel{E}_T the reconstruction of sparticle masses appears to be less problematic than that in the SM.

Another characteristic signature the model under consideration is the direct decays of sparticles other than the LSP into lepton number violating channels. Apparently the stringent constraints on the RPV couplings obtained from the neutrino data (see below) suggest that the branching ratios(BRs) of these decays will be highly suppressed compared to the competing RPC decays. One notable exception is the direct RPV decay of the lighter top squark [6, 7, 8, 9], if it happens to be the next to lightest supersymmetric particle(NLSP). This assumption is theoretically well-motivated due to large mixing effects in the top squark mass matrix. In this case the RPC decays of the top squark are also suppressed (to be elaborated later) and can naturally compete with the RPV decays even if the underlying couplings are as small as that required by the neutrino data. Thus the competition among different decay modes of the lighter top squark, which may be observed during Tevatron RUN II, is a hallmark of RPV models of neutrino mass [9].

Of course the see saw mechanism [10] which can be naturally implemented in any grand unified theory(GUT) not necessarily supersymmetric, provides an elegant alternative explanation of small neutrino masses. Unfortunately the simplest version of this theory, a GUT

with a grand desert, predicts a low energy spectrum practically identical with that of the SM. Thus there is no testable prediction outside the neutrino sector.

In view of the large number of RPV parameters, constraints on them [3, 11] are usually obtained from the experimental data by employing a simplifying assumption. It is assumed that only a minimal set of the parameters contributing to the observables under study are numerically significant. Following this approach one usually analyzes some benchmark scenarios, each consisting of a minimal set of RPV parameters at the weak scale [12, 13], capable of reproducing a phenomenologically viable neutrino mass matrix. Constraints on the parameters belonging to each scenario are then obtained by using the neutrino oscillation data [12, 13].

Among the examples in Ref. [12], we have focused on a specific model with three trilinear couplings λ'_{i33} (where $i = 1,2,3$ is the lepton generation index) and three bilinear RPV parameters μ_i . The stringent upper bounds on the trilinear (bilinear) couplings are $\sim 10^{-4}$ ($\sim 10^{-4} GeV$). As a result the contributions of these couplings to most low energy processes except LSP decays are negligible. As already mentioned, a notable exception could be the direct RPV decay of the lighter top squark [8, 9] into a b -quark and a charged lepton. Moreover, by reconstructing the lepton - jet invariant mass the lepton number violating nature of the decay can be directly established [9]. A model independent estimate of the minimum observable branching ratio (MOBR) of the channel $\tilde{t}_1 \rightarrow e^+ \bar{d}$ as a function of the lighter top squark mass ($m_{\tilde{t}_1}$) for Tevatron RUN II was also presented [9]. This estimate was then translated into the magnitudes of the λ 's for representative values of the parameters in the RPC sector and they were found to be close to the bounds obtained from the oscillation data.

In this paper we go a step beyond simple estimates and obtain testable quantitative predictions. We find various combinations of three λ' -type couplings allowed by the neutrino data. We do this by randomly generating 10^9 sets of the above six RPV couplings for representative values of the parameters in the RPC sector and identify the sets consistent with the oscillation data [14]. Our numerical results are checked by analytical calculations in a simple approximation (see sections 2 and 3 for the details). An interesting common feature of all the allowed sets is that one μ_i is much smaller than the other two and for each such scenario there are two characteristic patterns of the λ'_{i33} couplings. We thus have six generic scenarios. In each scenario the relative BRs of the three decay modes $\tilde{t}_1 \rightarrow l_j^+ \bar{b}$ reflect the underlying model. Thus if some of the RPV decay channels of \tilde{t}_1 are observed with BRs as predicted, a particular generic scenario can be vindicated. Of course more definite conclusion can be drawn if complementary information about the RPC sector, the masses of the sparticles in particular, can be obtained kinematically (by measuring invariant masses of the final state particles, edges of the energy distributions of some of the decay products etc). Some simple examples will be given later.

In our numerical work, we have chosen the parameters of the RPC sector corresponding to several scenarios classified according to the properties of the electroweak gaugino sector which determine the tree level neutrino masses (see section 4 for the details). In each case the lightest neutralino is assumed to be the LSP. We then study the predicted competition among various RPC [15, 16] and RPV decay modes of the top squark NLSP for RPV couplings allowed by the neutrino data. We find that many of the solutions predict BRs larger than

the estimated MOBR at Tevatron in [9]. We have also calculated the number of some typical signal events, where the expected background is low from top squark production and decay at Tevatron RUN II and LHC.

If on the other hand no signal is seen during Tevatron RUN II the allowed parameter space (APS) will be significantly squeezed. From the limits on the trilinear couplings obtained from Tevatron RUN I and RUN II [8] and from the projected sensitivity of RUN II data to these couplings [9], it seems that $\lambda'_{i33} \sim 10^{-4}$ can be ruled out for lighter top squark masses within the kinematic reach of the Tevatron.

If the top squark is not the NLSP and the RPV couplings are as small as that required by the current neutrino data [14], the decay of the LSP would be the only signature of the RPV model of neutrino mass. However, the amount of information that may be extracted will depend on parameters of the RPC sector, in particular on the LSP mass. If the LSP is lighter than the top quark, then it decays via the modes

$$\tilde{\chi}_1^0 \rightarrow \nu_l b \bar{b} \quad (1)$$

where $l = e, \mu$ or τ . Since the neutrinos are not detectable the branching ratios of the individual channels can not be measured. The decay length of the LSP depends on many model parameters belonging to the RPC and RPV sectors and pin pointing the underlying model of neutrino mass from one observable may not be an easy task (see, however, [17]). In addition the lepton number violating nature of the underlying interaction can not be directly established since the neutrinos escape the detector.

The signatures will be unambiguous if the $\tilde{\chi}_1^0$ happens to be heavier than the top quark. In this case apart from the decay channel in Eq. (1) the LSP will also decay into a charged lepton (e, μ or τ), the top quark and the anti-bottom quark, a clearly lepton number violating signature. This observation motivates us to also scan the parameter space where the LSP is heavier than the top quark. Of course the decay modes involving the top quark will be phase space suppressed compared to the ones in Eq. (1). Nevertheless our computations show that the branching ratios of the three modes involving the t-quark are numerically significant over the entire parameter space allowed by the oscillation constraints. Since the LSP is rather heavy in this scenario it is unlikely to be produced at the Tevatron. However, observation of all four modes and measurement of their branching ratios at the LHC or ILC will provide crucial tests of the underlying model of neutrino mass. We have calculated the size of some typical signals from the production of electroweak gaugino pairs at the LHC.

The plan of the paper is as follows. In section 2 we establish the notations and briefly review the neutrino mass matrix in the RPV model under study. In section 3 we identify the six generic scenarios of the RPV sector compatible with the neutrino data and using several representative values of the parameters of the RPC sector obtain sets of RPV parameters allowed by the oscillation data. In section 4 the top squark decays are studied in different scenarios. The LSP decays are analyzed in section 5. Our conclusions and future outlooks are summarized in section 6.

2. Neutrino mass matrix at the tree and loop level

R-parity is a multiplicative quantum number defined as follows [3],

$$R_p = (-1)^{3B+L+2S}, \quad (2)$$

where B is the baryon number, L is the lepton-number and S denotes the spin. For particles $R_p = +1$ and for sparticles $R_p = -1$.

In general the superpotential of the MSSM may contain RPV terms which violate both B and L conservation. This leads to catastrophic proton decay with a mean life time not allowed experimentally. All B and L violating terms can be removed from the superpotential by imposing R-parity as a symmetry. The resulting model is known as the R-parity conserving MSSM. In order to prevent proton decay it is, however, sufficient to remove either B-violating or L-violating terms by imposing appropriate discrete symmetries. Models with B-violating terms only can not generate neutrino masses. As discussed in the introduction we have focused on a specific model of neutrino mass with λ' type couplings only. The general R-parity violating superpotential of our interest takes the form:

$$W = W_{MSSM} + W_{\mathcal{R}_p}, \quad (3)$$

$$W_{\mathcal{R}_p} = \lambda'_{ijk} \epsilon_{ab} L_i^a Q_j^b D_k^c + \mu_i \epsilon_{ab} L_i^a H_2^b. \quad (4)$$

Here, W_{MSSM} [2] is the usual superpotential of the MSSM containing the terms which give mass to the SM fermions. The $i, j, k = 1, 2, 3$ are generation indices and $a, b = 1, 2$ are $SU(2)$ indices and 'c' denotes charge conjugation. The λ' 's are dimensionless trilinear RPV Yukawa like couplings, μ_i 's are bilinear RPV terms [3, 18] with dimensions of mass, which determines the amount of mixing between the lepton and Higgs superfields. In Eq.(4) L , Q and H_2 denote, respectively, $SU(2)_L$ doublet lepton, quark and up type higgs superfields and D is the $SU(2)_L$ singlet down type quark superfields. One can also construct models of ν -mass with RPV λ -type couplings [3, 4, 5, 19] only. The phenomenology of such models will be quite distinct from that discussed in this paper.

The tree level and loop level neutrino mass matrices are given below [3, 5, 12]:

$$\mathcal{M}_{\nu_{ij}}^{\text{tree}} = C \mu_i \mu_j, \quad (5)$$

and C is given by :

$$C = g_2^2 \frac{(M_1 + \tan^2 \theta_W M_2)}{4 \det M} v_d^2 \quad (6)$$

where g_2 is the $SU(2)$ gauge coupling, M_1, M_2 are the $U(1)$ and $SU(2)$ gaugino masses respectively and $\det M$ is the determinant of the R-parity conserving neutralino mass matrix. Here we are working in the basis where the sneutrino vacuum expectation values (vevs) are zero, $v = \sqrt{v_d^2 + v_u^2}$, where v_d (v_u) is the vev of down (up) type Higgs field. The one loop mass matrix is given by :

$$\mathcal{M}_\nu^{\text{loop}} = \begin{pmatrix} K_2 \lambda_{133}^{\prime 2} & K_2 \lambda'_{133} \lambda'_{233} & K_2 \lambda'_{133} \lambda'_{333} \\ K_2 \lambda'_{133} \lambda'_{233} & K_2 \lambda_{233}^{\prime 2} & K_2 \lambda'_{233} \lambda'_{333} \\ K_2 \lambda'_{133} \lambda'_{333} & K_2 \lambda'_{233} \lambda'_{333} & K_2 \lambda_{333}^{\prime 2} \end{pmatrix}, \quad (7)$$

where K_2 is given by :

$$K_2 = 3 \frac{X_b}{16\pi^2} \frac{f(x_q)}{M_{q2}^{(3)^2}} (m_b^2). \quad (8)$$

with

$$f(x) = -\frac{\ln x}{1-x}, \quad x_q = \left(\frac{M_{q1}^{(3)}}{M_{q2}^{(3)}} \right)^2 \text{ and} \quad (9)$$

$$X_b = A_b - \mu \tan \beta. \quad (10)$$

In the above X_b is the off-diagonal mixing term in the b-squark mass matrix , A_b is the soft trilinear term for the bottom squarks, $\tan \beta$ is the ratio of v_u to v_d , μ is the higgsino mass parameter , m_b is mass of the bottom quark . $M_{q1,q2}^{(3)}$ are the masses of the two b - squark mass eigenstates.

In this work we shall assume that the masses of the right handed and left handed squarks are equal. The same assumption applies to the slepton sector.

Thus, we take mass matrix up to the one-loop to be

$$\mathcal{M}_\nu = \mathcal{M}_\nu^{\text{tree}} + \mathcal{M}_\nu^{\text{loop}}. \quad (11)$$

It has been noted in the literature that there may be other loop contributions to the neutrino mass matrix [20, 5]. For example, the soft breaking RPV bilinear terms may contribute to some of the loops [5]. As has already been mentioned the large number of free parameters compels one to work in benchmark scenarios with a limited number of RPV parameters.

In Table [1] we present the neutrino data that has been used for the numerical work in this paper [14]. We shall consider the data at the 2σ level. The notations used are as follows [21]: the neutrino mass squared differences are $\Delta_{sol}^2 = \Delta m_{21}^2 = |m_2^2 - m_1^2|$ and $\Delta_{atm}^2 = \Delta m_{31}^2 = |m_3^2 - m_1^2|$ respectively, where m_1 , m_2 and m_3 are the three eigenvalues of the neutrino mass matrix in Eq. 1 [12]. The mixing angles are extracted from the eigenvectors corresponding to appropriate mass eigenvalues.

3.The six generic scenarios allowed by neutrino data

The neutrino mass matrix in section 2 can be recasted in the following form:

parameter	best fit	2σ	3σ	4σ
$\Delta m_{sol}^2 [10^{-5} eV^2]$	8.1	7.5–8.7	7.2–9.1	7.0–9.4
$\Delta m_{atm}^2 [10^{-5} eV^2]$	2.2	1.7–2.9	1.4–3.3	1.1–3.7
$\sin^2 \theta_{12}$	0.30	0.25–0.34	0.23–0.38	0.21–0.41
$\sin^2 \theta_{23}$	0.50	0.38–0.64	0.34–0.68	0.30–0.72
$\sin^2 \theta_{13}$	0.000	≤ 0.028	≤ 0.047	≤ 0.068

Table 1: Best-fit values, 2σ , 3σ , and 4σ intervals for the three flavour neutrino oscillation parameters from global data analysis [14] including solar, atmospheric, reactor (KamLAND and CHOOZ) and accelerator (K2K) experiments [1].

$$\mathcal{M}_\nu = \begin{pmatrix} D_1 & T_1 & T_2 \\ T_1 & D_2 & T_3 \\ T_2 & T_3 & D_3 \end{pmatrix}, \quad (12)$$

where T_i and D_i are given below :

$$D_1 = C\mu_i^2 + K_2\lambda_{133}^2 \quad (13)$$

$$D_2 = C\mu_i^2 + K_2\lambda_{233}^2 \quad (14)$$

$$D_3 = C\mu_i^2 + K_2\lambda_{333}^2 \quad (15)$$

$$T_1 = C\mu_1\mu_2 + K_2\lambda'_{133}\lambda'_{233} \quad (16)$$

$$T_2 = C\mu_1\mu_3 + K_2\lambda'_{133}\lambda'_{333} \quad (17)$$

$$T_3 = C\mu_2\mu_3 + K_2\lambda'_{233}\lambda'_{333} \quad (18)$$

The oscillation parameters can be easily calculated analytically if any one of the T_i s vanish and $D_i \neq 0$ for all i . Thus we tentatively propose the following generic scenarios :

(a) $\mu_1 = 0$ and either $\lambda'_{233} = 0$ ($T_1 = 0$) or $\lambda'_{333} = 0$ ($T_2 = 0$)

(b) $\mu_2 = 0$ and either $\lambda'_{133} = 0$ ($T_1 = 0$) or $\lambda'_{333} = 0$ ($T_3 = 0$)

(c) $\mu_3 = 0$ and either $\lambda'_{133} = 0$ ($T_2 = 0$) or $\lambda'_{233} = 0$ ($T_3 = 0$)

The above patterns help us to classify different regions of the RPV parameter space consistent with the oscillation data in Table [1].

For illustration we consider a particular hierarchy $\mu_1 \ll \mu_2$ or μ_3 (generic scenario (a)) and the following representative choice of RPC parameters : $M_1=110$, $M_2=200$, $\mu=400$, $\tan\beta=5$, $M_{\tilde{q}}=400$, $A_{\tilde{q}}=1000$ where all masses and mass parameters are in GeV. We randomly vary all six RPV parameters within the ranges shown in Table [2] columns 2 and 3 and generate 10^9 sets of parameters. Only μ_1 is constrained to be rather small.

We then pick up one solution corresponding to $\mu_1 = 0.08 \times 10^4 eV$, $\mu_2 = 140 \times 10^4 eV$, $\mu_3 = 111 \times 10^4 eV$, $\lambda'_{133} = 3.94 \times 10^{-5}$, $\lambda'_{233} = .015 \times 10^{-5}$ and $\lambda'_{333} = 7.03 \times 10^{-5}$. The numerically calculated oscillation parameters are presented in the second column of Table [3]. In column

RPV parameters	Given ranges		Allowed ranges	
	Max	Min	Max	Min
$\mu_1[10^4 eV]$	50.0	0.001	19.0	0.10
$\mu_2[10^4 eV]$	300.0	1.0	134.0	90.0
$\mu_3[10^4 eV]$	300.0	1.0	178.0	89.0
$\lambda'_{133}[10^{-5}]$	12.0	0.001	4.32	3.2
$\lambda'_{233}[10^{-5}]$	12.0	0.001	9.52	0.01
$\lambda'_{333}[10^{-5}]$	12.0	0.001	9.67	0.002

Table 2: Allowed ranges of RPV parameters in scenario (a)

3 of the same table we present the analytically calculated results with the approximation $\mu_1 = 0$, $\lambda'_{233} = 0$, while other RPV parameters are as above. The agreement between the two sets provides a test of the reliability of the numerical procedure. Changing the range of variation of μ_1 does not lead to any qualitatively new solution with μ_1 comparable to μ_2 or μ_3 . Thus classifying a generic scenario by a small magnitude of μ_1 is indeed valid.

Neutrino oscillation parameters	Numerical results	Analytical results
$\Delta m_{sol}^2 [10^{-5} eV^2]$	8.65	8.80
$\Delta m_{atm}^2 [10^{-3} eV^2]$	1.74	1.69
$\sin^2 \theta_{12}$	0.329	0.327
$\sin^2 \theta_{23}$	0.437	0.435
$\sin^2 \theta_{13}$	0.016	0.016

Table 3: Comparison of Numerical and Analytical results

Out of 10^9 sets of randomly generated RPV parameters only a few satisfy the data in Table [1]. This illustrates the highly restrictive power of the currently available oscillation data inspite of the relatively large errors. The allowed ranges of the six RPV parameters are presented in Table [2] columns 4 and 5. Examining the entire APS corresponding to the hierarchy $\mu_1 \ll \mu_2, \mu_3$, where μ_2, μ_3 can be comparable, one can identify two subclasses under the generic scenario (a). The trilinear RPV couplings in the two subclasses are found to satisfy the following patterns:

$$(a_1) \lambda'_{333} > \lambda'_{133} \geq \lambda'_{233},$$

$$(a_2) \lambda'_{233} > \lambda'_{133} \geq \lambda'_{333}.$$

In fact most of the APS a_1 (a_2) corresponds to $\lambda'_{233} \ll \lambda'_{133}$ ($\lambda'_{333} \ll \lambda'_{133}$). However, there are exceptions albeit for relatively small regions of the APS, where the two smaller couplings could be of comparable magnitude.

For $\mu_2 \ll \mu_1$ or μ_3 (scenario b) and $\mu_3 \ll \mu_1$ or μ_2 (scenario c) each region of the APS is also characterized by a specific pattern of the trilinear couplings due to the constraints imposed by the neutrino data. If some direct RPV decay modes are observed, these patterns would be reflected in the measured BRs revealing the model underlying neutrino oscillations.

For $\mu_2 \ll \mu_1$ or μ_3 , the trilinear couplings follow the patterns

$$\begin{aligned} (b_1) \quad & \lambda'_{133} \approx \lambda'_{233} \gg \lambda'_{333}, \\ (b_2) \quad & \lambda'_{233} > \lambda'_{333} \gg \lambda'_{133}. \end{aligned}$$

For $\mu_3 \ll \mu_1$ or μ_2 , on the other hand, we have

$$\begin{aligned} (c_1) \quad & \lambda'_{333} > \lambda'_{133} \gg \lambda'_{233}, \\ (c_2) \quad & \lambda'_{333} > \lambda'_{233} \gg \lambda'_{133}. \end{aligned}$$

It can be readily checked analytically that even in the most general case when none of the RPV parameters vanish one eigenvalue is still zero. Thus analytical solutions are still possible. The formulae for the masses and the mixing angles are somewhat cumbersome. For scanning the parameter space we therefore prefer the numerical method.

It should be noted that there is no straightforward way of determining the μ_i parameters directly from collider signals. Thus it is gratifying to note that the scenarios (a_1) - (c_2) can be identified by the decay branching ratios alone provided RPV decays into charged leptons are observed.

On the face of it the scenarios (a_1) and (c_1) look similar. But scanning the entire APS in both cases we have found that

$$2.6 \% < BR(e) < 4.2 \% \text{ and } 19.7 \% < BR(\tau) < 10.2 \% \text{ in } (a_1),$$

while

$$9.5 \% < BR(e) < 12.8 \% \text{ and } 18.4 \% < BR(\tau) < 22.0 \% \text{ in } (c_1),$$

where $BR(e)$ ($BR(\tau)$) refer to the BR of any direct RPV decay mode into a final state with e (τ). Thus each scenario will have its characteristic decay pattern.

4. The lighter top squark decay

We now study the collider signals that may be triggered by the sets of λ' couplings consistent with the neutrino data[14]. The signals can be classified into a few patterns corresponding to the six generic scenarios discussed in section 3 and the hierarchy of trilinear couplings associated with them. All allowed sets would lead to the RPV decays of the lighter top squark (\tilde{t}_1) in Eq. (19) with appreciable branching ratios if it happens to be the NLSP, which is the case over a large region of the RPC parameter space.

$$(a) \quad \tilde{t}_1 \rightarrow l_i^+ b \quad (19)$$

where $i = 1 - 3$. From section 3 it is clear that the relative BRs of the three leptonic modes will be different in generic scenarios a1) - c2). Hence identification of the RPV parameters underlying the model of neutrino mass in future experiments is a distinct possibility.

The RPC decay modes of the lighter top- squark (\tilde{t}_1) are listed below :

$$(b) \quad \tilde{t}_1 \rightarrow b\tilde{\chi}_1^+ \quad (20)$$

$$(c) \quad \tilde{t}_1 \rightarrow b\ell\tilde{\nu}, b\tilde{\ell}\nu, bW\tilde{\chi}_1^0 \quad (21)$$

$$(d) \quad \tilde{t}_1 \rightarrow c\tilde{\chi}_1^0 \quad (22)$$

$$(e) \quad \tilde{t}_1 \rightarrow b\tilde{\chi}_1^0 f\bar{f}' \quad (23)$$

f and \bar{f}' being a quark-antiquark or $l-\bar{l}$ pair. If the lighter top squark is the NLSP, only the decay modes d) and e) and the last mode of c) are allowed. The mode in c) will be phase space suppressed for \tilde{t}_1 masses within the kinematic reach of the Tevatron, which are the main subject of this study. Moreover, it will be highly suppressed if the LSP happens to be bino like, which is quite natural in popular models like the ones with a unified gaugino mass. We shall not consider this mode in this paper. The channels in d) and e) have naturally suppressed widths and can very well compete with each other [16] or with the RPV mode, especially if λ'_{i33} is $\sim 10^{-4} - 10^{-5}$ as required by neutrino data [8, 9].

Our choices of the RPC parameters are guided by the gaugino sector. It is clear from Eq.(5) section 2 that the parameter C sets the scale of the tree level neutrino mass matrix. This C depends solely on the parameters of the gaugino mass matrices. Accordingly we have chosen the following scenarios.

1. Models in which the lighter chargino ($\tilde{\chi}_1^\pm$) and the two lighter neutralinos ($\tilde{\chi}_1^0$ and $\tilde{\chi}_2^0$) are higgsino like ($M_1, M_2 \gg \mu$) and all have approximately the same mass ($\approx \mu$). Thus it is difficult to accommodate the top squark NLSP without fine adjustments of the parameters. Thus the LSP decay seems to be the only viable collider signature which will be discussed in the next section.
2. Models in which $\tilde{\chi}_1^\pm$, $\tilde{\chi}_1^0$ and $\tilde{\chi}_2^0$ are gaugino like ($M_1 < M_2 \ll \mu$) and the top squark is the NLSP.
3. Models in which $\tilde{\chi}_1^\pm$ and $\tilde{\chi}_2^0$ are mixed ($M_1 < M_2 \approx \mu$) and the top squark is the NLSP.

In all models the parameters are so chosen that the lightest neutralino ($\tilde{\chi}_1^0$) happens to be the LSP. Further the squarks belonging to the right and left sectors of all flavours are assumed to be mass degenerate. In fact although the common squark mass, μ and $\tan \beta$ occur in both the neutrino and the top squark sector, one can choose the soft trilinear parameter A_t , which does not affect the neutrino sector, to satisfy the top squark NLSP criterion in most cases. However, attention must be paid so that large values of A_t do not lead to a charge color breaking (CCB) vacuum [22]. The BRs of top the squark decay

modes and competition among the RPV and RPC decays would be highly indicative of the underlying model.

For model 2, the gaugino like model, we use the following representative values of the parameters of the RPC sector: $M_1 = 110$, $M_2 = 200$, $\mu = 400$, $\tan\beta = 5$, $M_{\tilde{q}} = 400$, $A_b = 1000$, $A_t = 970$ and $M_A = 300$ where all masses and mass parameters are in GeV and M_A is the CP odd higgs mass. The first six parameters, which are the same as the ones used in section 3 for numerical illustration, along with the RPV parameters determine neutrino masses and mixing angles(see section 2). The last two parameters are required to realize the top squark NLSP condition and the CCB condition respectively. It should be noted that the BR of the loop decay increases significantly for larger M_A .

Top squark NLSPs having different masses are realized varying A_t . For this set of RPC parameters the NLSP and the CCB conditions are satisfied for $940 < A_t < 980$. In addition we have used a common mass of L and R type sleptons $M_{\tilde{l}} = 350$ and $A_\tau = 1000$ for the computation of the BRs of the RPC modes.

We then randomly generate 10^8 sets of the six RPV parameters in scenarios (a_1 and a_2) and filter out the ones allowed by the data in Table [1]. As discussed in section 3 in all allowed sets there is one dominant coupling (λ'_{233} or λ'_{333}). This hierarchy will obviously be reflected in the observed BRs. In Fig. 1 we present the BR of each of the three competing decay modes in Eq.(19) (including all leptonic channels), Eq.(22) and Eq.(23) (including all possible f and \bar{f}' combinations) and the corresponding number of allowed solutions out of 10^8 randomly generated parameter sets. This figure clearly illustrates the competition among the three decay modes of the top squark NLSP. Here $A_t = 970\text{GeV}$ and $m_{\tilde{t}_1} = 181.5\text{GeV}$. The RPV decay modes do not dominate although the combined BR of the three RPV modes is appreciable (20 % - 30 %) over most of the APS. It also follows from this figure that the number of solutions allowed by the ν - data is indeed a tiny fraction of the total number of generated parameter sets. Thus the available oscillation data is already very resistive in spite of the large errors.

In Ref.[9] top squark pair production followed by their RPV decays into e^+e^- or $\mu^+\mu^-$ channels were studied for Tevatron RUN II. The minimum observable BR (MOBR) at Tevatron for the decays into the e or μ channel have been estimated as a function of $m_{\tilde{t}_1}$. For $m_{\tilde{t}_1} = 181.5\text{GeV}$ the MOBR of the ($\tilde{t}_1 \rightarrow e^+b$) or ($\tilde{t}_1 \rightarrow \mu^+b$) channel is approximately 20 %

It may be recalled that the analysis of [9] was conservative since only the leading order top squark pair production cross section and a total integrated luminosity of only 2000pb^{-1} were used. The next to leading order cross section is about 30% larger and accordingly a smaller estimate of the MOBR is expected. The total integrated luminosity during RUN II may be as large as 9000pb^{-1} [23] which can further lower the MOBR. An improvement in the observability of RPV decays is also expected if ee , $\mu\mu$ and $e\mu$ channels are simultaneously analyzed.

For the solutions in which decays into the τ lepton dominate, the combined BR of the modes involving lighter leptons are below the MOBR. Since this happens in a large region of the APS, it will be worthwhile to estimate the MOBR of this channel. On the other hand if the RPV decay into e or μ dominates, many allowed solutions have BRs close to the MOBR estimated in [9].

For numerical illustrations we have considered the following points in the APS

- A) $\lambda'_{133} = 3.72 \times 10^{-5}$, $\lambda'_{233} = 3.3 \times 10^{-5}$ and $\lambda'_{333} = 8.5 \times 10^{-5}$ (scenario (a_1), $\lambda'_{133} \approx \lambda'_{233}$)
- B) $\lambda'_{133} = 4.2 \times 10^{-5}$, $\lambda'_{233} = 1.3 \times 10^{-5}$ and $\lambda'_{333} = 8.3 \times 10^{-5}$ (scenario (a_1), $\lambda'_{133} > \lambda'_{233}$)
- C) $\lambda'_{133} = 4.2 \times 10^{-5}$, $\lambda'_{233} = 8.6 \times 10^{-5}$ and $\lambda'_{333} = 1.8 \times 10^{-5}$ (scenario (a_2), $\lambda'_{233} > \lambda'_{333}$)

The BRs of top squark decay modes into different leptonic channels for the parameter sets A) - C) are given in Table [4].

Decay modes	$\tilde{t}_1 \rightarrow e^+b$	$\tilde{t}_1 \rightarrow \mu^+b$	$\tilde{t}_1 \rightarrow \tau^+b$	loop	4 body
BR(A)	0.03	0.024	0.158	0.69	0.10
BR(B)	0.04	0.004	0.153	0.70	0.11
BR(C)	0.039	0.163	0.007	0.69	0.10

Table 4: BRs of the competing decay modes of the lighter top squark in the gaugino dominated model (Model 2, see text for the choice of parameters)

In Table [5] we present the number of events corresponding to different dileptonic final states at the Tevatron arising from RPV decays of both the produced top squarks. The number of events are computed for the BRs in Table [4], $\sqrt{s} = 2$ TeV and an integrated luminosity of 9000 pb^{-1} . For $m_{\tilde{t}_1} = 181.5$ GeV the production cross section $\sigma(p\bar{p} \rightarrow \tilde{t}_1\tilde{t}_1^*)$ is 0.41 pb as computed by CalcHEP v2.1 [24]. The signal

$$\tilde{t}_1\tilde{t}_1^* \rightarrow l_i^+\bar{b}l_j^-b \quad (24)$$

is abbreviated as L_{ij} , where $i,j = 1,2,3$ for e, μ and τ respectively. For $i \neq j$ we considered dileptons of all charge combinations.

	L_{11}	L_{12}	L_{13}	L_{22}	L_{23}	L_{33}
# of events (A)	3	5	34	2	27	91
# of events (B)	5	1	44	0	4	86
# of events (C)	5	46	2	97	8	0

Table 5: Typical sizes of opposite sign dileptons of different flavour combinations at the Tevatron from top squark pair production using the BRs in Table [4].

It is expected that the backgrounds can be suppressed to the desired level by employing standard kinematical cuts, b-tagging and by reconstructing the invariant masses of the two top squarks [9].

Another interesting signal arises if one of the produced top squarks decay via an RPV mode (a) while the other decays via the loop induced mode Eq. (22) followed by the LSP

decay leading to

$$\tilde{t}_1 \tilde{t}_1^* \rightarrow l_i^+ b c \nu b \bar{b} \text{ or } l_i^- \bar{b} \bar{c} \nu b \bar{b} \quad (25)$$

where $i=1,2,3$ as before and L_i denotes the above signal. The number of signal events for different i are presented in Table [6] using the same inputs as in Table [5]. We have included leptons of both signs in the signal.

	L_1	L_2	L_3
# of events (A)	152	121	804
# of events (B)	206	20	789
# of events (C)	198	829	35

Table 6: Typical sizes of various signals from top squark pair production at Tevatron RUN II when one of them decays into a RPV channel while the other into the loop induced mode followed by LSP decay.

The top squark mass can be reconstructed by the invariant masses of the two hardest leptons and jets [9] in any L_{ij} type event. The upper edge of the invariant mass spectrum of the two jets with lowest and next to lowest energy in any L_i type signal may provide information about the LSP mass.

If the parameter K_2 , which sets the scale of the one loop mass matrix, is decreased keeping the parameters of the gaugino sector fixed, the allowed values of λ'_{i33} couplings increase and apparently larger BRs of the RPV modes are allowed. However, we shall illustrate the constrained nature of the model in the next paragraph and show that the above BRs cannot be arbitrarily large inspite of many free RPC parameters in the model.

The parameter K_2 decreases for higher values of the common squark mass. In practice for a fixed set of gaugino parameters the common squark mass cannot be increased significantly without violating the top squark NLSP condition. Of course larger values of the A_t parameter may restore the NLSP condition. But larger values of A_t tend to violate the CCB condition. Finally the parameter M_A can be increased to satisfy the CCB condition but as noted earlier that would enhance the loop decay width as well and the BRs of the RPV modes will still be suppressed. Thus once we know the parameters of the gaugino sector from complementary experiments and observe RPV decays of the top squark NLSP, the predicted BR of these modes cannot be made arbitrarily large by adjusting the common squark mass or M_A .

The BR of the RPV decays increase significantly if we consider model 3 with mixed $\tilde{\chi}_1^\pm$ and $\tilde{\chi}_2^0$. In this case the parameter C increases substantially compared to its typical magnitude in model 2 while the loop level mass matrix has a smaller K_2 due to a smaller higgsino mass parameter μ . Thus the loop level mass matrix can be effective only for larger values of the trilinear RPV couplings.

We demonstrate these effects with the same parameter set as above except that we take $\mu = 210.0$ GeV. We present the corresponding histogram in Fig. 2. It follows that the entire APS correspond to larger BRs of the RPV modes (including all leptonic channels).

For illustrating the signals at the LHC we consider a new parameter space leading to a heavier top squark NLSP beyond the reach of the Tevatron. We have chosen $m_{\tilde{t}_1} = 350.65$ GeV, $M_1 = 310$, $M_2 = 400$, $\mu = 800$, $\tan\beta = 5$, $M_{\tilde{q}} = 550$, $M_{\tilde{l}} = 450$, $A_b = 1000$, $A_\tau = 1000$, $A_t = 1350$ and $M_A = 500$ where all masses and mass parameters are in GeV. At the LHC the top squark pair production cross section is 4.28 pb for this $m_{\tilde{t}_1}$.

We have chosen the following sets of RPV parameters consistent with the ν data which reflects the same characteristics as in A) - C) listed above.

A) $\lambda'_{133} = 2.92 \times 10^{-5}$, $\lambda'_{233} = 2.27 \times 10^{-5}$ and $\lambda'_{333} = 6.27 \times 10^{-5}$

B) $\lambda'_{133} = 3.4 \times 10^{-5}$, $\lambda'_{233} = 6.6 \times 10^{-5}$ and $\lambda'_{333} = 1.83 \times 10^{-5}$

C) $\lambda'_{133} = 3.39 \times 10^{-5}$, $\lambda'_{233} = 1.92 \times 10^{-5}$ and $\lambda'_{333} = 6.48 \times 10^{-5}$

The corresponding BRs are shown in Table [7].

Decay modes	$\tilde{t}_1 \rightarrow e^+b$	$\tilde{t}_1 \rightarrow \mu^+b$	$\tilde{t}_1 \rightarrow \tau^+b$	loop	4 body
BR(A)	0.12	0.075	0.57	0.23	0.001
BR(B)	0.16	0.59	0.045	0.21	0.001
BR(C)	0.16	0.05	0.58	0.21	0.001

Table 7: BRs of different decay modes of the lighter top squark in Model 2 (see text for the choice of parameters)

Using the BRs in Table [7] and a representative integrated luminosity of $30 fb^{-1}$ one can easily calculate the number of various signal events. For example, we obtain 44696 L_{22} and 31817 L_2 events with the parameter set B.

5. LSP decay

As discussed in the introduction unless $m_{\tilde{\chi}_1^0} > m_t$, LSP decay alone cannot provide detailed information about the underlying model of m_ν .

Of course the decay of the LSP into the channel in Eq. (1) may provide circumstantial evidences in favour of an underlying RPV model of neutrino mass. For example, if $\tilde{\chi}_1^0$ is assumed to be the LSP, then $\tilde{\chi}_1^+ \tilde{\chi}_1^-$ and $\tilde{\chi}_1^+ \tilde{\chi}_1^0$ production followed by appropriate decay chains ending in LSP decays are indicative of an underlying model of neutrino mass [25]. In Ref. [25] the prospect of observing this signal at RUN II was studied. It was concluded that this signature can be probed up to $m_{1/2} = 230$ GeV(320 GeV) with an integrated luminosity of $2 fb^{-1}$ ($30 fb^{-1}$). Here $m_{1/2}$ is the common gaugino mass at the GUT scale. However, the lepton number violating nature of the decay can not be established by the data.

It may be noted that the pure RPC decay $\tilde{\chi}_2^0 \rightarrow \tilde{\chi}_1^0 b\bar{b}$, which may have a large BR if one of the bottom squark mass eigenstates happens to be lighter than the other squarks at large $\tan\beta$, has collider signatures very similar to the decay of Eq.(1). This is especially so if the LSP mass is much smaller than $m_{\tilde{\chi}_2^0}$ which is quite common in models with non-universal gaugino masses. Thus one has to worry about the possibility of RPC SUSY faking the RPV signal.

Using model 1) (see section 4) we have chosen the following of RPC parameters :
 $M_1 = 710$, $M_2 = 800$, $\mu = 395$, $\tan\beta = 5$, $M_{\tilde{q}} = 500$, $M_{\tilde{l}} = 450$, $A_b = 1000$, $A_\tau = 1000$,
 $A_t = 800$ and $M_A = 300$ where all masses and mass parameters are in GeV. This leads to
 $m_{\tilde{t}_1} = 391$ GeV and $m_{\tilde{\chi}_1^0} = 388$ GeV Since $m_{\tilde{\chi}_1^0} > m_t$ the following additional decay modes
open up :

$$(a) \tilde{\chi}_1^0 \rightarrow e \bar{b} t \quad (26)$$

$$(b) \tilde{\chi}_1^0 \rightarrow \mu \bar{b} t \quad (27)$$

$$(c) \tilde{\chi}_1^0 \rightarrow \tau \bar{b} t \quad (28)$$

In Fig. 3 we present the BRs of the four competing decay modes of the LSP and the corresponding number of allowed solutions out of 10^8 sets of randomly generated RPV parameters.

From the sets allowed by the neutrino data we have chosen the following RPV parameters : $\lambda'_{133} = 5.43 \times 10^{-5}$, $\lambda'_{233} = 10.19 \times 10^{-5}$, $\lambda'_{333} = 0.87 \times 10^{-5}$. The resulting BRs are presented in column 2 of Table [8]. Here, the three neutrinos carry the \cancel{E}_T .

Decay modes	BR (%)in Higgsino model	BR (%)in Gaugino model
$\tilde{\chi}_1^0 \rightarrow \cancel{E}_T b \bar{b}$	12.5	79.7
$\tilde{\chi}_1^0 \rightarrow t e \bar{b}$	19.3	3.7
$\tilde{\chi}_1^0 \rightarrow t \mu \bar{b}$	67.7	16.2
$\tilde{\chi}_1^0 \rightarrow t \tau \bar{b}$	0.5	0.4

Table 8: BRs of different decay modes of the LSP in higgsino dominated model (Model 1) and the gaugino dominated model (Model 2) (see text for the choice of parameters).

We next compare this result with the gaugino dominated scenario (Model 2). We choose $M_1 = 388$, $M_2 = 500$, $\mu = 800$ and $A_t = 870$ keeping all other RPC parameters same as that in the Higgsino type model. The choice of parameters is dictated by the fact that the masses of the LSP and different squarks remain practically the same in the two models being compared. The BRs in this model are presented in the last column of Table [8] The BRs of the modes involving charged leptons and the t quark are significantly enhanced in the Higgsino model because of the large top Yukawa coupling.

We next study gaugino pair production followed by cascade decays with RPC and RPV parameters as in model(1) quoted above. We consider the following signal

$$G_\alpha G_\beta \rightarrow l_i^{(\mp)} l_j^{(\mp)} \bar{b} \bar{b} t t X \quad (29)$$

where $G_\alpha G_\beta$ represents any pair of electroweak gauginos , $i, j = 1, 2, 3$ for e , μ and τ respectively, L_{ij} represents the number of this signal and X denotes any other particles produced. The number of signal events from different gaugino pair production at LHC are presented in Table [9]. The production cross-sections involved are calculated using CalcHEP v2.1 [24]. L_{12} includes e and μ events with all possible charge combinations and $L_{11/22}$ represents events with same sign di-leptons only.

In Fig. 4 we present the LSP decay length vs the number of allowed solutions in Model 1. It is seen that apart from a small region of the APS the decay will be inside the detector.

Gaugino pair	σ (pb)	L_{11}	L_{22}	L_{12}
$\tilde{\chi}_1^0 \tilde{\chi}_2^0$	18.5×10^{-3}	206	2551	5808
$\tilde{\chi}_1^+ \tilde{\chi}_1^-$	68.2×10^{-3}	762	9405	21416
$\tilde{\chi}_1^- \tilde{\chi}_2^0$	10.2×10^{-3}	113	1406	3200
$\tilde{\chi}_1^+ \tilde{\chi}_2^0$	23.4×10^{-3}	261	3226	7348
$\tilde{\chi}_1^0 \tilde{\chi}_1^-$	10.6×10^{-3}	118	1461	3328
$\tilde{\chi}_1^0 \tilde{\chi}_1^+$	24.6×10^{-3}	274	3392	7724

Table 9: Number of L_{11}, L_{22} and L_{12} events (see text) arising from various gaugino pair production at LHC followed by LSP decay

6. Conclusions

In this paper we have studied the APS of the RPV parameters in a model of neutrino mass subject to the constraints imposed by the neutrino oscillation data [14]. The model we have considered has three bilinear RPV couplings μ_i and three trilinear couplings λ'_{i33} , where i is the lepton index, and we work in a basis where the sneutrino vev is zero. As expected from the upper bounds on the λ'_{i33} couplings obtained by the earlier analyses [12], we find for representative choice of the RPC parameters, the allowed magnitudes of these couplings are indeed very small (see section 3). Our analyses reveal that even the currently available ν -oscillation data with relatively large errors are quite restrictive. Out of many randomly generated sets of RPV parameters consistent with the upperbounds on them [12], only a few are allowed by the data.

Moreover, we also identify six generic scenarios, consistent with neutrino data, leading to distinctive collider signatures. These scenarios are listed as $a_1) - c_2)$ in section 3. In each scenario there is one small bilinear parameter μ_i and a characteristic hierarchy of λ'_{i33} couplings. Thus if a few direct RPV decay modes of any sparticle are observed their relative BRs would reflect the underlying model of neutrino mass. We have studied the decay modes of the top squark NLSP both at Tevatron RUN II and at the LHC (section 4). Over the entire APS the BRs of the RPV decays are found to be significant for representative values of the RPC parameters and the hierarchy among them can potentially reveal the underlying model of neutrino mass. The LSP decays can provide similar information if the LSP mass is larger than m_t (section 5).

Hopefully RPV decays in the above channels will be seen at hadron colliders and at least some parameters of the RPC sector can be measured kinematically (some examples are discussed in section 4). The accurate measurement of the relative BRs at the ILC will then provide an exciting program for probing the origin of neutrino mass.

In this paper we have chosen a particular set of RPV parameters in the physical basis at the weak scale for explaining the current ν - oscillation data. Following the standard practice we have further assumed that the magnitudes of all other RPV parameters are negligible. There is, however, another exciting possibility. Let a few relatively large RPV parameters not directly related to the ν - sector, be generated at a high scale (say M_{GUT}) by any suitable

mechanism (for examples by effective operators [26]). The renormalization group (RG) evolution of these parameters down to the weak scale can then generate the parameters μ_i and λ'_{i33} having magnitudes severely suppressed compared to the input parameters [?]. This happens due to the flavour violation (non-diagonal Yukawa couplings matrices) inevitably present in the quark sector. It was shown in [27, 28] that any three input couplings at M_{GUT} with different lepton indices chosen from λ'_{i13} and λ'_{i23} , $i=1,2,3$, can induce a viable ν - mass matrix at the weak scale. Thus at the weak scale there may be some relatively large λ' couplings in addition to the small parameters underlying ν - physics. Moreover when the quark mass matrices are diagonalized at the weak scale rotations on the quark fields may further generate new RPV couplings [28] relevant for ν - physics from the above relatively large λ' - type couplings. Of Course such rotations may also induce other λ' -type couplings leading to unacceptable flavour changing neutral currents [29]. Care should, therefore, be taken in choosing the input parameters at M_{GUT} . Because of the relatively large λ' - type couplings the RPV collider phenomenology and some rare decays of K-mesons and τ -leptons would be rather spectacular in these models. Several specific models and their associated phenomenologies were discussed with numerical illustrations in [28].

Acknowledgment:

SPD acknowledges support from the project (SP/S2/K-10/2001) of the Department of Science and Technology (DST), India. AD acknowledges support from the project (SR/S2/HEP-18/2003) of the DST, India. SP's work was supported by a fellowship from Council of Scientific and Industrial Research (CSIR), India.

References

- [1] B. T. Cleveland *et al.*, Astrophysical. Jori. **496**, 505 (1998); W. Hampel *et al.* [GALLEX Collaboration], Phys. Lett. B **447**, 127 (1999); M. Apollonio *et al.* [CHOOZ Collaboration], Phys. Lett. B **466**, 415 (1999) Eur. Phys. J. C **27**, 331 (2003); M. Altmann *et al.* [GNO Collaboration], Phys. Lett. B **490**, 16 (2000); Q. R. Ahmad *et al.* [SNO Collaboration], Phys. Rev. Lett. **87**, 071301 (2001), Phys. Rev. Lett. **89**, 011301 (2002), Phys. Rev. Lett. **89**, 011302 (2002); J. N. Abdurashitov *et al.* [SAGE Collaboration]; J. Exp. Theor. Phys. **95** (2002) 181; S. Fukuda *et al.* [Super-Kamiokande Collaboration], Phys. Lett. B **539**, 179 (2002); *ibid*, Phys. Rev. Lett. **89**, 011301 (2002); K. Eguchi *et al.* [KamLAND Collaboration], Phys. Rev. Lett. **90**, 021802 (2003); M.H. Ahn, [K2K Collaboration] Phys. Rev. Lett. **90**, 041801 (2003); M. C. Gonzalez-Garcia, review talk given at 10th International Conference on Supersymmetry and Unification of Fundamental Interactions (SUSY02), Hamburg, Germany, 17-23 June 2002, eprint hep-ph/0211054.
- [2] For reviews on Supersymmetry, see, *e.g.*, H. P. Nilles, Phys. Rep. **1**, 110 (1984); H. E. Haber and G. Kane, Phys. Rep. **117**, 75 (1985) ; J. Wess and J. Bagger, *Supersymmetry and Supergravity*, 2nd ed., (Princeton, 1991); M. Drees, P. Roy and R. M. Godbole, *Theory and Phenomenology of Sparticles*, (World Scientific, Singapore, 2005).

- [3] For reviews on RPV SUSY see, *e.g.*, H.K. Dreiner, in *Perspectives on Supersymmetry*, ed. G.L. Kane, World Scientific (hep-ph/9707435); A.Barbier *et al.*, Phys. Rep. **420**, 1 (2005) (hep-ph/0406039); M. Chemtob, Prog. Part. Nucl. Phys. **54**, 71 (2005) (hep-ph/04060290).
- [4] C. S. Aulakh and R. N. Mohapatra, Phys. Lett. B **119**, 136 (1982); L. Hall and M. Suzuki, Nucl. Phys. B **231**, 419 (1984); J. Ellis *et al.*, Phys. Lett. B **150**, 142 (1985); G. Ross and J. Valle, Phys. Lett. B **151**, 375 (1985); S. Dawson, Nucl. Phys. B **261**, 297 (1985); Y.Grossmann and H.E. Haber, Phys. Rev. Lett. **78**, 3438 (1997), Phys. Rev. D **79**, 093008 (1999).
- [5] For a recent review and further references see, *e.g.*, S. Rakshit, Mod. Phys. Lett. A19, 2239(2004).
- [6] Aseshkrishna Datta and B. Mukhopadhyaya, Phys. Rev. Lett. **85**, 248 (2000); D. Restrepo, W. Porod and J. W. F. Valle, Phys. Rev. D **64**, 055011 (2001).
- [7] CDF collaboration (D. Acosta *et al.*), Phys. Rev. Lett. **92**, 051803 (2004).
- [8] S. Chakrabarti, M. Guchait and N. K. Mondal, Phys. Rev. D **68**, 015005 (2003); Phys. Lett. **B600**, 231 (2004).
- [9] S. P. Das, Amitava Datta and M. Guchait, Phys. Rev. D **70**, 015009 (2004).
- [10] M. Gell-Mann, P. Ramond, and R. Slansky, in *Supergravity*, ed. D. Freedman and P. van Nieuwenhuizen (North-Holland, Amsterdam, 1979), p. 315; T. Yanagida, in *Proc. of the Workshop on Unified Theory and Baryon Number in the Universe*, ed. O. Sawada and A. Sugamoto (KEK, Japan, 1979); R. Mohapatra and G. Senjanovic, Phys. Rev. Lett. **44**, 912 (1980), Phys. Rev. D **23**, 165 (1981).
- [11] V. Barger, G. F. Giudice and T. Han, Phys. Rev. D **40**, 2987 (1989); G. Bhattacharyya, (hep-ph/9709395); B.C. Allanach, A. Dedes and H.K. Dreiner, Phys. Rev. D **D60**, 075014 (1999). All bounds on λ and λ' -type couplings have been reviewed by F. Ledroit and G. Sajot, GDR-S-008 (ISN, Grenoble,1998). See: http://qcd.th.u-psud.fr/GDR_SUSY/GDR_SUSY_PUBLIC/entete_note_publicue.
- [12] A.Abada, M. Losada, Phys. Lett. B **492**, 310 (2000).
- [13] A. Abada, G. Bhattacharyya and M. Losada, Phys. Rev. D **66**, 071701(R) (2002).
- [14] For recent global analyses of neutrino oscillation data, see, *e.g.*, M. Maltoni *et al.*, New. J. Phys **6**, 122 (2004); A. Bandyopadhyay *et al.*, Phys. Lett. B **608**, 115 (2005). G. L. Fogli *et al.* hep-ph/0506083
- [15] K.I. Hikasa and M. Kobayashi Phys. Rev. D **36**, 724 (1987).
- [16] C. Boehm, A. Djouadi and Y. Mambrini, Phys. Rev. D **61**, 095006 (2000).
- [17] F. de Campos *et al.*, Phys. Rev. D **71**, 075001 (2005).

- [18] See also, C.H. Chang and Tai-Fu Feng, Eur. Phys. J. C **12**, 137 (2000).
- [19] See also, M. Bisset, O.C.W. Kong, C. Macesanu and L. H. Orr, Phys. Lett. B **430**, 274 (1998).
- [20] See Y. Grossman and H. E. Haber in [4]; M. Hirsch, H. V. Klapdor-Kleingrothaus and S. G. Kovalenko, Phys. Lett. B **98**, 311 (1997); S. Davidson and M. Losada, Phys. Rev. D **65**, 075025 (2002); F. Borzumati and J. S. Lee, Phys. Rev. D **66**, 115012 (2002); Y. Grossman and S. Rakshit, Phys. Rev. D **69**, 093002 (2004).
- [21] G. Altarelli and F. Feruglio, New. J. Phys **6**, 106 (2004).
- [22] S. Raby, A. Lleyda and C. Munoz Nucl. Phys. B **471**, 3 (1996) and references therein.
- [23] See, *e.g.*, V. Buscher, (hep-ex/0411063).
- [24] See, *e.g.*, A. Pukhov, CalcHEP—a package for evaluation of Feynman diagrams and integration over multi-particle phase space see: <http://www.ifh.de/pukhov/calchep.html>.
- [25] V. Barger, T. Han, S. Hasselbach and D. Marfatia, Phys. Lett. B **538**, 346 (2002).
- [26] See, *e.g.*, L.J. Hall and M. Suzuki, Nucl. Phys. B **231**, 419 (1984), D.E. Brahm and L.J. Hall, Phys. Rev. D **40**, 2449 (1989) and K. Tamvakis, Phys. Lett. B **382**, 251 (1996).
- [27] See, B.C. Allanach, A. Dedes and H.K. Dreiner, Phys. Rev. D **69**, 115002 (2004).
- [28] See, A. Datta, J.P. Saha, A. Kundu and A. Samanta, Phys. Rev. D **72**, 055007 (2005).
- [29] K. Agashe, M. Graesser, Phys. Rev. D **54**, 4445 (1996).

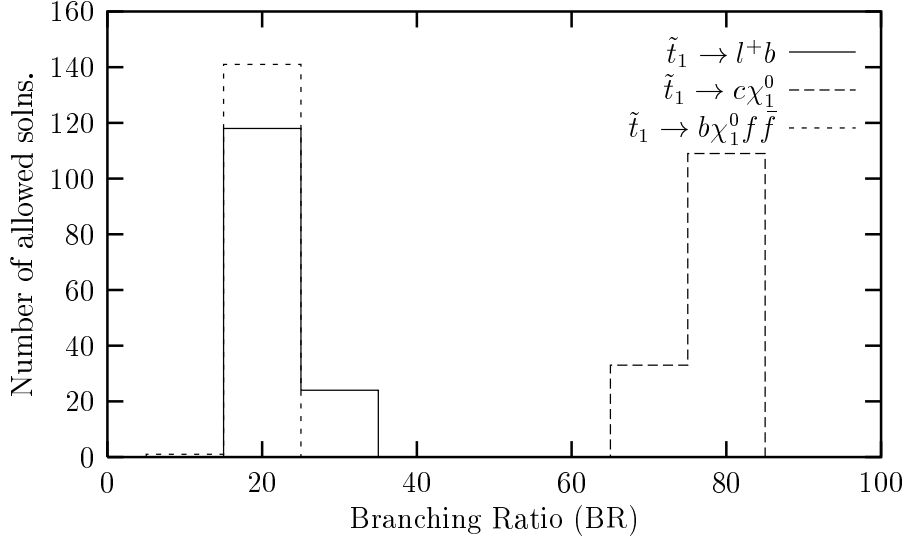


Figure 1: The branching ratios(%) of the three competing decay modes vs the number of allowed solutions in Model 2 (see text for the parameters used).

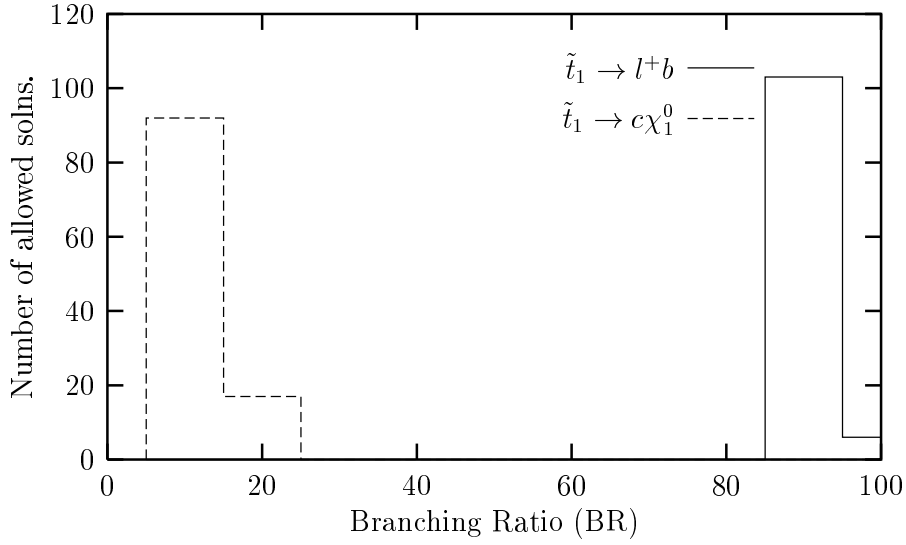


Figure 2: The branching ratios(%) of the two competing decay modes vs the number of allowed solutions in Model 3 (see text for the parameters used).

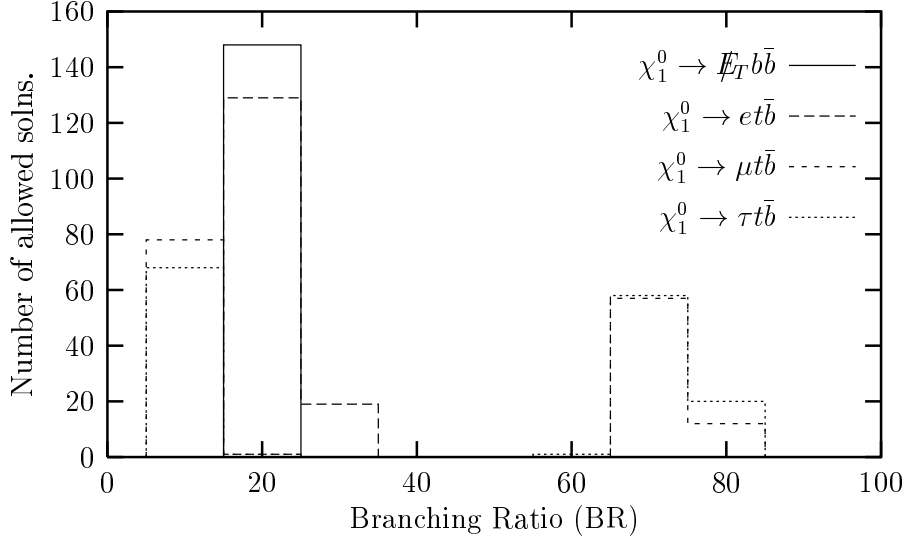


Figure 3: The branching ratios (%) of competing LSP decay modes vs the number of allowed solutions in Model 1 (see the text for the parameters used).

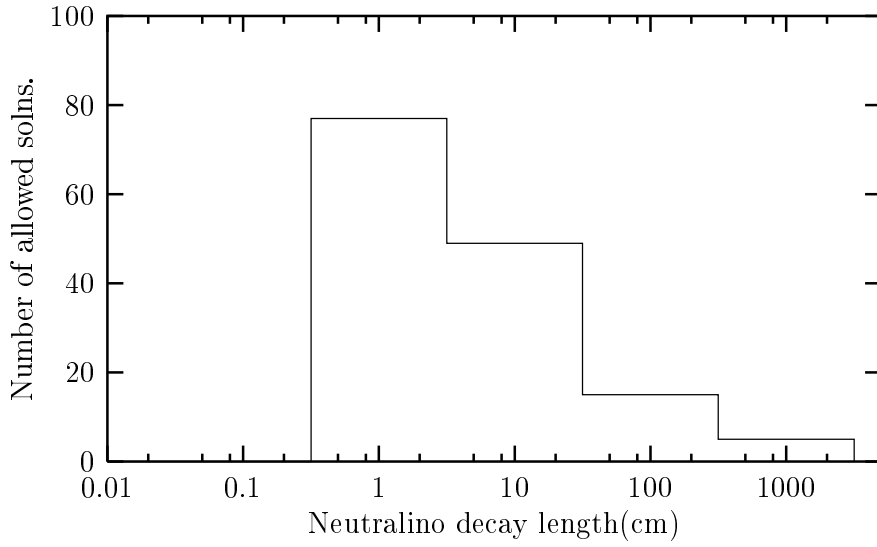


Figure 4: Neutralino decay length vs the number of allowed solutions in Model 1 (see the text for the parameters used).